Experimental analysis of the effect of initial conditions on spontaneous detonation development mechanisms for a hydrogen/n-decane mixture

Roseline Ngozi Ezekwesili[ab], Marc Bellenoue[a], Camille Strozzi[a], Myles Bohon[b]
[a] Pprime Laboratory,[b] TU Berlin
[a]Poitiers, Vienne, France,[b]Berlin, Germany

1 Introduction

Current combustion technologies are evolving. Modern spark ignition engines have been downsized and boosted resulting in much higher compression ratios. Moreover, new combustion methods such as pistonless Constant Volume Combustion (CVC) - which is a subsonic implementation of Pressure Gain Combustion (PGC) technology - have been introduced [1]. The development of unwanted detonations remains a challenge in both boosted spark ignition engines and CVC technology. These unwanted detonations cause mechanical damage and reduce efficiency. Unwanted detonations can develop by the Shock Wave Amplification by Coherent Energy Release (SWACER) mechanism explained by Lee et al [2]. The SWACER mechanism states that if a reactivity gradient exists in the end-gas which is reactive enough to autoignite, sequential autoignition of neighboring pockets of gas can produce an autoignition wave. At low reactivity gradients, the heat release from pockets of gas autoigniting can generate a leading pressure wave if the mixture is sufficiently energetic. If the autoignition wave is in phase with the leading pressure wave, the heat release from the autoignition wave can feed into the pressure wave, reinforcing it and resulting in a transition to detonation. Due to inhomogeneities in the fuel-oxidizer mixing procedure, spots of increased reactivity, termed hotspots, will always exist in practical applications. A reactivity gradient will exist across these hotspots making the system susceptible to detonation transition by the SWACER mechanism. Alongside the SWACER mechanism, it was also found that under certain conditions, autoignition occurred at the end wall of the chamber [3]. End wall autoignition can also give rise to detonation development through the Shockwave Reflection Induced Detonation (SWRID) Mechanism [3] where pressure waves reflecting from the chamber wall couple with the heat release from the local end wall autoignition.

Several works [4-8] highlighted the fact that the competition between deflagration and autoignition plays a key role in whether a transition to detonation occurs or not. A propagating deflagration compresses the end-gas until it becomes “auto-ignitable” meaning that it attains temperatures high enough to autoignite. Zhang et al [5] showed that at elevated flame speeds, in the time between the end-gas becoming “auto-ignitable” and actually autoigniting, the deflagration consumed all the fresh gas thus suppressing a transition to detonation. The Burnt Mass Fraction (BMF) quantifies the amount of unburnt gas remaining in the combustion chamber at a given time. The higher the BMF, the lower the proportion of unburnt gas remaining in the chamber. In [6,7] it was found that the BMF at the time when the end-gas first becomes auto-ignitable is not only a determinant in whether a transition to detonation occurs but also determines the intensity of any resulting pressure oscillations.

Mixing hydrogen with jet fuels can be considered as a realistic first step towards decarbonizing the air transport industry. N-decane has been found to have properties similar to kerosene but with a far simpler chemistry [9], therefore studying H_2/n-decane mixtures will provide a useful insight into the detonation development properties of hydrogen/jet fuel mixtures. The influence of the H_2 amount in the fuel mixture

Correspondence to: r.ezekwesili@tu-berlin.de

was studied by the authors in similar conditions in [13] and the present work is focused on how initial temperature and pressure conditions impact the deflagration-autoignition competition and the development of end wall autoignition for a fuel of n-decane with 5% H_2 in the fuel mixture by mass.

2 Experimental set-up and numerical tools

The Modular Deflagration Autoignition Detonation (MDAID) combustion chamber shown in figure 1d was used in the present work.

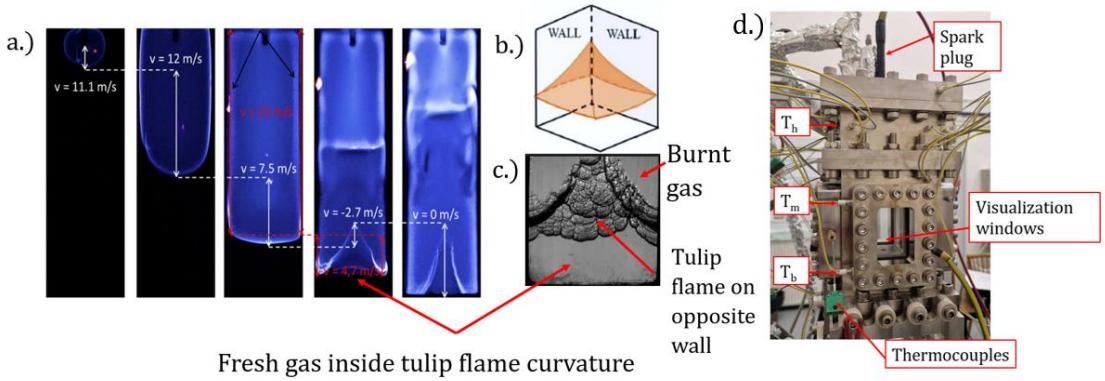

Figure 1: a.) Example of a tulip flame formation in a 120 mm chamber [12]. The top of the chamber corresponds to the upper chamber wall, b.) A schematic drawing of the tulip flame structure [12], c.) A schlieren image of a tulip flame for a stoichiometric $C_{10}H_{22}/O_2/Ar$ mixture, d.) Experimental MDAID chamber used in present study.

The combustion chamber has internal dimensions of 40 x 40 x 172 mm^3 and sets of heating cartridges, each controlled by 3-zone PID-regulators, were placed at the top, middle and bottom of the chamber. Thermocouples mechanically fastened into the chamber walls monitor the wall temperature. By setting the PID-regulators to different set-points, a temperature gradient is imposed on the gas within the chamber. To find the corresponding gas temperature, in a separate test, a cap fixed to a K-thermocouple with a 7.6 µm wire was mounted to the top wall of the chamber, the chamber was heated to the experimental configuration and the temperature was taken every 5 mm on a vertical axis between the bottom wall of the chamber (henceforth referred to as the end wall) and a vertical distance of 130 mm above the end wall. For the experiments, the cap was replaced by a spark plug mounted to the top wall of the chamber, the chamber was filled with the fuel-air premixture and the spark plug was ignited delivering an energy discharge of approximately 30 millijoules which initiated a deflagration. Due to hydrodynamic processes, deflagrations propagating in a closed tube will eventually form an inverted flame front curvature called a tulip flame [10] as shown in figures 1a,1b, and 1c. The unburnt gas within this tulip flame pocket is considered to experience conditions comparable to adiabatic compression. The resulting deflagration propagated down the chamber, evolved into a tulip flame and compressed the unburnt gas to a temperature high enough to autoignite. The subsequent combustion processes were observed through 40 x 60 mm UV quartz windows located at the bottom of the chamber.

A high-speed photron SAZ camera with a capture speed of 80,000 frames per second and an ultra-high-speed Shimadzu HPVX2 camera running at capture speeds between 500,000 and 2,000,000 frames per second, were used to capture schlieren images of the resulting combustion regimes which usually occurred in the first 45 mm from the end wall of the chamber. A piezo electric pressure sensor (Kistler 6152CU20) mounted at the end wall monitored the pressure evolution of the chamber with a cut-off frequency of 70 kHz. In this present work, a $5\%H_2/C_{10}H_{22}/O_2/Ar$ stoichiometric mixture was investigated where the percentage refers to a fuel mass percentage. A 5% H_2 fuel mass percentage corresponds to a 78.8% molar fuel percentage. As the molar composition determines the chemical

behaviour, this mixture provided a good insight into the effects of mixing hydrogen with n-decane. The mixture composition is shown in equation 1.

$$3.71H_2 + C_{10}H_{22} + 17.36O_2 + 65.26Ar \quad (1)$$

The $H_2/O_2/Ar$ components of the mixtures were prepared in gaseous form in a pressurized bottle according to the partial pressure method. Liquid n-decane was injected via a syringe into the vacuumed heated chamber where it immediately vaporized. The gaseous mixture bottle was shaken to ensure mixing homogeneity between the low-density hydrogen and synthetic air. The gaseous mixture was then added slowly to the heated chamber to avoid re-condensation of the vaporized n-decane. The mixture composition was controlled through monitoring partial pressures with capacitive pressure sensors (MKS baratron 631). The heated chamber containing the complete premixture was left for 10 minutes to homogenize before the combustion was ignited with the spark plug. The standard heating configuration was top (T_h), middle (T_m) and bottom (T_b) thermocouple temperatures of 453 K, 455 K and 441 K respectively. At least 10 experiments were performed for each temperature gradient condition.

Numerical tools

The temperature evolution of the unburnt gas during the combustion processes could not be measured experimentally and was simulated using a variable volume reactor which simulated autoignition under adiabatic and variable volume conditions by following the experimental pressure evolution. All the numerical tools were built using the Cantera library and the mechanism selected was the n-decane Polimi mechanism [11].

3 Results and discussions

Figure 2 shows schlieren images of a typical combustion regime. As shown in this figure, the spark plug initiates a deflagration which evolves into a tulip flame compressing the unburnt gas to auto-ignitable conditions. N-decane is a long-chain hydrocarbon and experiences 2-stage ignition. The 1st stage ignition along the temperature gradient produces a cool flame and the more powerful 2nd stage ignition along the temperature gradient produces a Main Heat Release (MHR) wave, from which a transition to detonation can occur. At different instances in the combustion process, the unburnt gas will have different states. State 0 is the initial condition of the gas before spark plug ignition. The 1st stage ignition along the temperature gradient produces a cool flame as shown in Figure 2. The presence of a cool flame has been shown in [4] by Quintens et al when preforming experiments on n-decane mixtures in a similar experimental configuration. To verify that what was observed in the present experimental configuration was a cool flame, Planar Laser Induced Florescence (PLIF) analysis of the formaldehyde radical was performed. Moreover, the experimental delays between the cool flame and MHR onset were compared with the simulated delays between 1st stage and 2nd stage ignition simulated in the constant volume reactor. These analyses confirmed that the observed phenomenon was a cool flame. State II is the state of the gas just before the passage of the cool flame. State III is the state of the gas just before the passage of the MHR wave. In the following analysis, the temperature and pressure values presented at each state are the mean chamber properties averaged across all experiments. State properties are denoted by the state number as a subscript. An estimate of the BMF of the gas in the chamber was calculated using the formula shown in equation 2 where $P_{eq\text{-}ad}$ is the simulated constant volume, adiabatic equilibrium pressure (simulated with a constant volume reactor from state II conditions). P is the chamber pressure at a given instant and P_0 is the State 0 pressure. The lower the BMF, the higher the volume of unburnt gas remaining in the chamber.

$$BMF = \frac{P - P_0}{P_{eq-ad} - P_0} \quad (2)$$

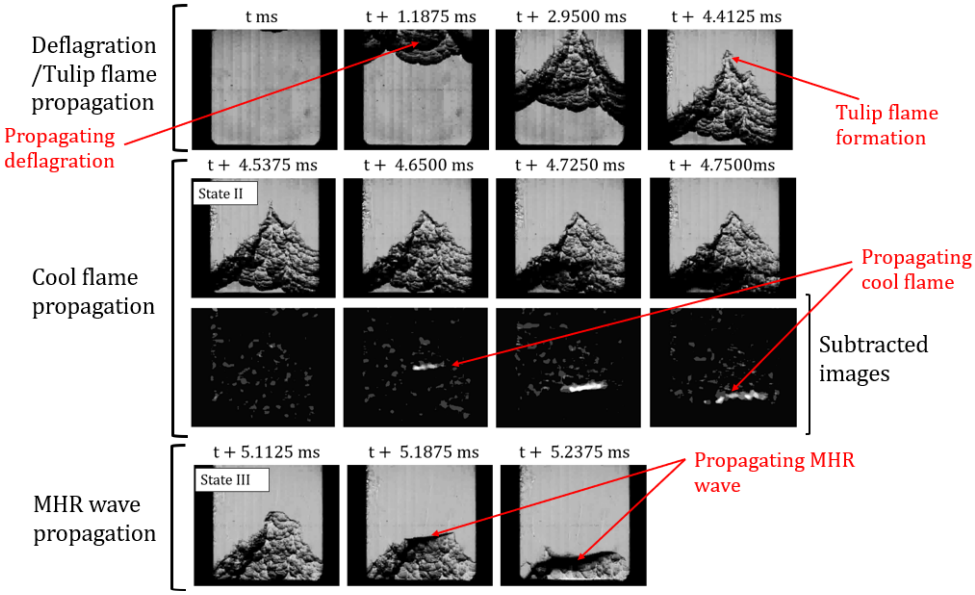

Figure 2: Schlieren images demonstrating the combustion regime for a stoichiometric 5%H_2/$C_{10}H_{22}$/O_2/Ar mixture initially at 3 bar and the standard heating configuration of T_h=453 K, T_m= 455 K and T_b = 441 K. The subtracted images are of 2 consecutive frames.

Changing initial temperature

Stoichiometric 5%H_2/$C_{10}H_{22}$/O_2/Ar mixtures initially at 3 bar were investigated at the standard heating configuration and at a heating configuration with the same initial temperature gradient but where all cartridge temperatures were 10 K lower. Table 1 summarizes the average properties at each state.

Table 1: properties at each state for stoichiometric 5%H_2/$C_{10}H_{22}$/O_2/Ar mixtures initially at 3 bar and different initial heating configurations

Initial temperature (K) (T_h,T_m,T_b)	**Detonation (%)**	**P_{II} (bar)**	**T_{II} (K)**	**BMF_{II}**	**BMF_{III}**
443,445,431 (Mean = 442 K)	100	19.2	772	0.81	0.86
453,455,441 (Mean = 452 K)	100	17.3	764	0.73	0.81

As seen in table 1, at the lower temperature condition, there is a higher BMF at each state meaning that relatively more unburnt gas has been consumed at the onset of each state. This is because at a lower initial temperature, a larger temperature raise and therefore more deflagration compression is required to bring the unburnt gas to the "auto-ignitable" temperature. The increased deflagration compression leads to more unburnt gas being consumed at each state, but the remaining unburnt gas is at a higher pressure. These properties however do not reduce the instances of transition to detonation when compared to the standard heating configuration condition. Figure 3 shows subtracted images of two consecutive frames of the unburnt gas during a transition to detonation for representative experiments from each heating condition. It is the compressed conditions which determine the autoignition wave properties, therefore the compressed temperature profile, just before autoignition, was simulated. These compressed temperatures do not cross into the NTC region. The MHR wave speed was characterized by tracking the local peaks in the schlieren images. It was found that the MHR wave accelerated at the domain positions of weak temperature gradient and this acceleration would continue until a detonation kernel would form at the MHR wave. This aligns with the behaviour observed by Quintens et al in [4] just before a transition to detonation via the SWACER mechanism. Therefore, it was hypothesized that detonation transition occurring at the MHR wave occurred by the SWACER mechanism. However, as seen in figure 3, at the standard heating configuration, an additional detonation transition mechanism

would occur where detonation kernels formed at the end wall at the same time the MHR wave was transitioning to detonation.

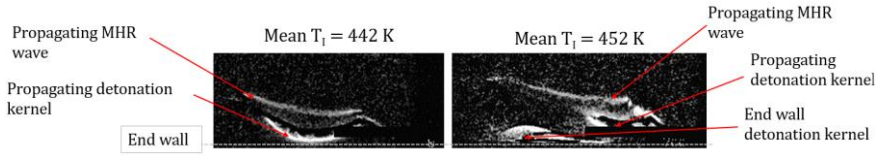

Figure 3: Subtracted (from two consecutive frames) and contrasted schlieren images during the detonation transition for 5%H_2/$C_{10}H_{22}$/O_2/Ar mixtures initially at 3 bar for a representative experiment from each heating condition.

Changing initial pressure

Stoichiometric 5%H_2/$C_{10}H_{22}$/O_2/Ar mixtures at the standard heating configuration with initial pressures of 2.0, 2.5 and 3.0 bar were investigated. Table 2 summarizes the average properties at each state.

Table 2: Properties at each state for stoichiometric 5%H_2/$C_{10}H_{22}$/O_2/Ar mixtures at the standard heating configuration and different initial pressures.

Initial Pressure (bar)	**Detonation (%)**	**P_{II} (bar)**	**T_{II} (K)**	**BMF_{II}**	**BMF_{III}**
2.0	0	11.6	766	0.75	
2.5	100	14.7	769	0.75	0.83
3.0	100	17.3	764	0.73	0.81

As shown in table 2, the state II temperatures and BMF values do not vary significantly across the different conditions. This is because gas auto-ignitability is more temperature than pressure dependent so roughly the same amount of unburnt gas is consumed by the deflagration to bring the unburnt gas to an auto-ignitable temperature. Despite the similar state II conditions, the instances of detonation transition go from 100% to 0 % between the 2.5 and 2 bar conditions. Figure 4 shows schlieren images at different times for representative experiments from each pressure group.

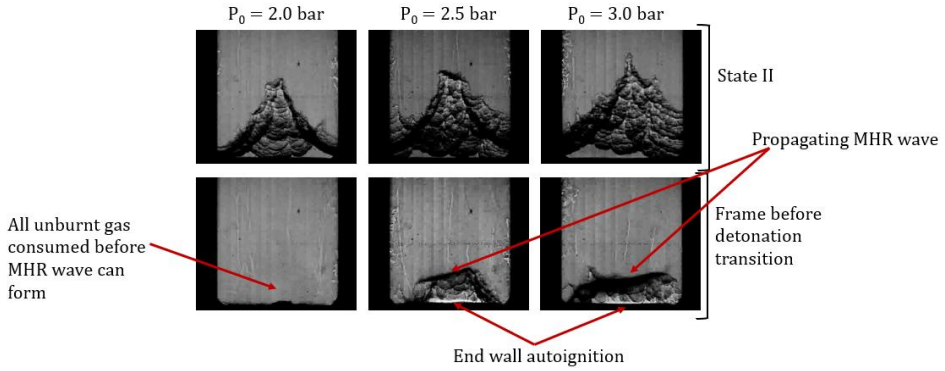

Figure 4: Images of the gas at different time points for stoichiometric 5%H_2/$C_{10}H_{22}$/O_2/Ar mixtures at different initial pressures and a heating configuration of T_h=453 K, T_m= 455 K, T_b = 441 K for a representative experiment from each pressure condition.

For the 2 bar condition, all the unburnt gas is consumed before an MHR wave can even form which suppresses any transition to detonation by the SWACER mechanism. This is because, due to the lower pressure at the point the gas becomes auto-ignitable, the delay between 1st and 2nd stage ignition is considerably larger when compared to the higher-pressure conditions. The delay between ignition stages is large enough that the deflagration is able to consume the remaining unburnt gas within this time. For both the 2.0 and 2.5 pressure conditions, end wall autoignition occurs in the frame before a transition to detonation was observed. At the standard heating configuration, whenever end wall autoignition was observed in the frame before detonation transition in the high-speed images, detonation kernels forming

at the end wall were observed in the ultra-high-speed images. Ultra-high-speed images were not available for the 2.5 bar pressure condition. However, from the autoignition at the end wall observed, it is strongly inferred that for this pressure condition, detonation kernels also developed at the end wall.

4 Conclusion

In conclusion, this study aimed to explore how changing the initial temperature and pressure could affect the deflagration autoignition competition and end wall autoignition for a stoichiometric $5\%H_2/C_{10}H_{22}/O_2/Ar$ mixture. It was found that changing the initial conditions did not affect the state II temperatures significantly. A lower initial temperature did not suppress detonations but resulted in a higher pressure and BMF at each state and did not result in end-gas autoignition. A lower initial pressure affected the autoignition deflagration competition enough to suppress a detonation. This was due to the different sensitivities of the two stages of autoignition to pressure. However, for the initial pressures where detonations did occur, end wall autoignition also occurred. Other results are not developed here for the sake of brevity: the effects of argon dilution, and equivalence ratio as well as the effects of the initial conditions on the resulting MHR autoignition wave properties were investigated. Moreover, the exact mechanism by which a transition to detonation occurred at each condition was found.

References

[1] Michalski Q, Boust B, Bellenoue M. (2019). Experimental investigation of ignition stability in a cyclic constant-volume combustion chamber featuring relevant conditions for air-breathing propulsion. Flow Turbul. Combust. 102:279.
[2] Lee JH, Knystautas R, Yoshikawa N. (1978). Photochemical initiation of gaseous detonations. Acta Astronaut. 5: 971
[3] Wang Z, Qi Y, Liu H, Zhang P, He X, Wang J. (2016). Shock wave reflection induced detonation under high pressure and temperature condition in closed cylinder. Shock Waves. 26: 687.
[4] Quintens H, Strozzi C, Zitoun R, Bellenoue M. (2020). Shock Waves. 30: 287.
[5] Zhang X, Wei H, Zhou L, Cai X, Deiterding R. (2020). Relationship of flame propagation and combustion mode transition of end-gas based on pressure wave in confined space. Combust. Flame. 214: 371.
[6] Yu H, Qi C, Chen Z. (2017). Effects of flame propagation speed and chamber size on end-gas autoignition. Proc. Combust. Inst. 46: 3533.
[7] Chen L, Wei H, Chen C, Feng D, Zhou L, Pan J. (2019). Numerical investigations on the effects of turbulence intensity on knocking combustion in a downsized gasoline engine. Energy. 166: 318.
[8] Ossman H, Strozzi C, Sotton J, Bellenoue M. (2023). Experimental and Numerical Study of Autoignition/Deflagration Transition Limit in an Optical Rapid Compression Machine. Combust. Sci. Technol.
[9] Alekseev VA, Soloviova-Sokolova JV, Matveev SS, Chechet IV, Matveev SG, Konnov AA. Laminar burning velocities of n-decane and binary kerosene surrogate mixture. 187: 429.
[10] Ponizy B, Claverie A, Veyssière B. (2014). Tulip flame - the mechanism of flame front inversion. Combust. Flame. 161: 3051.
[11] Ranzi E, Frassoldati A, Stagni A, Pelucchi M, Cuoci A, Faravelli T. (2014). Reduced Kinetic Schemes of Complex Reaction Systems: Fossil and Biomass-Derived Transportation Fuels. Int. J. Chem. Kinet. 46: 512.
[12] Quintens H, Strozzi C, Zitoun R, Bellenoue, M. (2019). Deflagration/Autoignition/Detonation Transition Induced by Flame Propagation in an N-Decane/O_2/Ar Mixture. Flow Turbul. Combust.. 102: 735.
[13] Ezekwesili R, Strozzi C, Bellenoue M, Weiss, A, Bohon M. (2025). Effect of Hydrogen and Residual Burned Gas addition to n-decane/O_2/Ar mixtures on the deflagration/autoignition/detonation transition in confined condition. [article in preparation].